THE ASTROPHYSICAL JOURNAL, 352:307–317, 1990 March 20

THE INFRARED CORONAL LINES OF RECENT NOVAE[1]

MATTHEW A. GREENHOUSE, G. L. GRASDALEN, C. E. WOODWARD, AND J. BENSON
Wyoming Infrared Observatory, University of Wyoming

R. D. GEHRZ
Department of Astronomy, University of Minnesota

E. ROSENTHAL[2]
Institute for Astronomy, University of Hawaii

AND

M. F. SKRUTSKIE
Five College Astronomy Program, Department of Physics and Astronomy, University of Massachusetts

Received 1989 April 19; accepted 1989 September 16

ABSTRACT

We report the discovery of infrared coronal emission lines in Nova V1819 Cyg and Nova V827 Her and present new high-resolution near-infrared spectra of coronal line emission in Nova QU Vul. These new results increase the number of known infrared coronal line novae from two to four and show that each of the four is characterized by approximately the same [Si VI]/[Si VII] line intensity ratio that reflects a common coronal zone electron temperature of approximately 3×10^5 K among these novae. Among the most interesting results of our study of novae is that each coronal line nova exhibits a remarkably similar near-infrared spectrum. This uniformity suggests that coronal line emission in novae will be only occasionally observed at optical wavelengths.

The abundance pattern for Al and Mg, is derived for two of the coronal line novae discussed, and the Ne abundance pattern is derived for QU Vul. We find that these novae are substantially overabundant in these elements. These data double the number of novae for which Al and Mg abundances have been determined. Observational evidence for novae outbursts on oxygen-neon-magnesium white dwarfs is increased as a consequence.

The first speckle interferometry of the coronal line emission region of a nova is presented. The coronal zone of QU Vul was spatially resolved at 0".6 using this technique in the 3.02 μm [Mg VIII] line. Comparison of our interferometry to high-resolution VLA maps of QU Vul suggests that the coronal line emission region encompasses the principal ejecta of the nova.

We present a new technique for interpreting the coronal line spectra that relates their infrared spectral evolution to electron temperature and density gradients in the expanding ejecta. The relative role of collisional ionization and photoionization in formation of the coronal species is discussed in detail. We find that photoionization alone cannot account for the observed ionization. Observational tests which will improve current understanding of the spectral evolution of novae and model constraints which result from these data are suggested.

Subject headings: infrared: spectra — interferometry — line identifications — stars: abundances — stars: novae

I. INTRODUCTION

Coronal emission lines of novae were first observed by Sanford (1946), who recorded emission lines of [Fe X] λ6374 and [Fe XIV] λ5303 on low-resolution photographic spectra of Nova T CrB (see § III*b* for a working definition of the term coronal line). During the years following this measurement, very high ionization states such as these were occasionally observed in optical spectra of novae (see, e.g., Gallagher and Starrfield 1978; Wallerstein and Garnavich 1986). The first infrared coronal lines were observed in Nova V1500 Cyg (Nova Cygni 1975) by Grasdalen and Joyce (1976). They found numerous emission lines of high ionization states of Al, Mg, and Si throughout the K (2.2 μm) and L (3.4 μm) atmospheric windows and concluded that the emission was produced in a coronal temperature gas which was substantially overabundant in aluminum relative to the Sun (Grasdalen and Joyce 1980). The idea that the near-infrared spectrum of novae could be dominated by overabundant highly ionized heavy metals was initially met with controversy (Black and Gallagher 1976). However, observations of other novae made in part with *IUE* during the years following V1500 Cyg revealed that very nonsolar abundance patterns are often observed among heavy elements such as Ne, Mg, and Al in novae ejecta (see, e.g., Williams *et al.* 1985; Snijders *et al.* 1987).

A program to regularly monitor novae over all ground-based infrared bands has been underway at the Wyoming Infrared Observatory (WIRO) for several years (see, e.g., Gehrz, Grasdalen, and Hackwell 1985; Gehrz *et al.* 1986; Greenhouse *et al.* 1988). This program revealed unusual [Ne II] 12.8 μm emission in Nova QU Vul (Nova Vulpeculae 1984 No. 2). Circular variable filter (CVF) spectra showed that the Ne emission was remarkable in both its intensity and line width, revealing an outflow velocity significantly in excess of

[1] Contribution 113 of the Wyoming Infrared Observatory.
[2] Visiting Astronomer, NASA Infrared Telescope Facility (IRTF), Mauna Kea, HI.

that predicted and observed for normal carbon-oxygen novae outbursts. The measured line strength remains the most intense [Ne II] emission observed in an astronomical object.

Recent models of novae occurring on oxygen-neon-magnesium (ONeMg) white dwarfs predict ejecta velocities and elemental abundances consistent with the neon emission observed in QU Vul and the aluminum emission observed in V1500 Cyg (Starrfield, Sparks, and Truran 1986; Truran and Livio 1986). This consistency and anomalous *L* band colors, discovered in QU Vul during routine broad-band photometry, prompted us to include low-resolution *K* and *L* band spectroscopy in our monitoring program which revealed coronal line emission in QU Vul (Greenhouse *et al.* 1988, hereafter Paper I). Since then, we have discovered the same emission in Nova V1819 Cyg (Nova Cygni 1986) and Nova V827 Her (Nova Herculis 1987) (Greenhouse 1987; Greenhouse *et al.* 1987). Three of the four known infrared coronal line novae were discovered by this program. No coronal line emission was found in Nova Vulpeculae 1987 (QV Vul). The spectrum of QV Vul does show an emission feature at 3.28 μm. A similar feature is observed in a variety of Galactic and extragalactic sources. Polycyclic aromatic hydrocarbon (PAH), quenched carbonaceous composite (QCC), and hydrogenated amorphous carbon (HAC) molecules have C—H vibrational stretch modes that can produce a similar feature at 3.28 μm (see, e.g., Allamandola, Tielens, and Barker 1987; Sakata *et al.* 1984; Duley and Williams 1986; Borghesi, Bussoletti, and Colaugeli 1987). More recently, we have begun to monitor the spatial development of novae shells and their coronal zones using speckle interferometry at continuum and coronal line wavelengths.

In the following sections, we discuss the origin of the coronal emission lines and the processes that form the ions and govern the spectral evolution of the coronal emission. We compare near-infrared spectra of two new coronal line novae to the spectrum of QU Vul described previously in Paper I and derive a coronal zone electron temperature for each nova. We also present new high-resolution *L* band spectra of QU Vul which constrain the temporal development of the ejecta velocity. Finally, we compare our speckle interferometry of QU Vul to VLA radio continuum maps of the nova.

II. OBSERVATIONS

a) *Near-Infrared CVF Spectra*

Low-resolution ($\lambda/\Delta\lambda = 40$) *K*-band spectra of Nova V1819 Cyg were taken on 1987 August 29 using the WIRO 234 cm telescope and InSb radiometer equipped with a *K* and *L* band CVF. Similar *K* band CVF observations of V827 Her were made on 1987 May 8 and August 29. Resolution $\lambda/\Delta\lambda = 75$ *L* band CVF observations of Nova QV Vul were made on 1988 April 21. Conventional beam switching 20″ north-south with a 6″ FWHM diaphragm was used in all cases. Absolute flux calibration was determined using α Lyr during April–July and β Peg during August. Zero-magnitude flux densities were derived from the WIRO photometric system described by Gehrz, Grasdalen, and Hackwell (1987). The CVF spectra were spectrally oversampled by at least a factor of 4 during each measurement. We estimate the uncertainty in wavelength calibration of the spectra to be ± 0.01 μm as a result of the oversampling. Wavelength calibration of the CVF was determined by observation of NGC 7027, HD 193793, and IRAS 2122+5050 (see, respectively, Smith, Larson, and Fink 1981; Lambert and Hinkle 1984; and de Muizon *et al.* 1986).

The spectra of V1819 Cyg, V827 Her, and QV Vul are shown in Figure 1. The spectrum of QU Vul shown in Paper I is reproduced in Figure 1 for convenience. In contrast to QU Vul, the *L* band spectrum of QV Vul exhibits a steep continuum with an emission feature at 3.28 μm. Hyland and McGre-

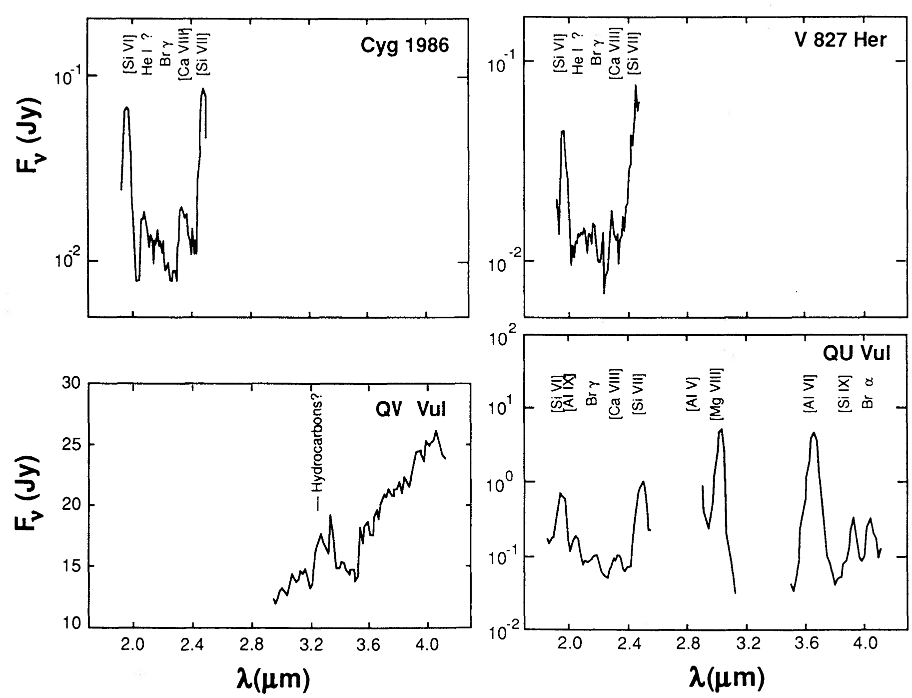

FIG. 1.—The near-infrared spectrum of Nova Cygni 1986, Nova V827 Her, Nova QV Vul, and Nova QU Vul. The dates of observation, spectral resolution, and uncertainties are discussed in § II*a*. Line identifications shown are listed in more detail in Table 1.

TABLE 1

THE CORONAL LINES OF RECENT NOVAE

Ion	Transition	μ (μm)	E_T (eV)
Ca VIII	$^2P^o(3/2, 1/2)$	2.32	127.1
Al V	$^2P(1/2, 3/2)$	2.88	120.0
Ne VI	$^2P(1/2, 3/2)$	7.60	126.2
Al VI	$^3P(1, 2)$	3.66	153.8
Si VI	$^2P(1/2, 3/2)$	1.96	166.8
Si VII	$^3P^o(1, 2)$	2.47	205.1
Mg VIII	$^2P^o(3/2, 1/2)$	3.02	225.0
Al IX	$^2P^o(3/2, 1/2)$	2.04	284.6
Si IX	$^3P(1, 0)$	3.92	401.4

TABLE 2

PEAK LINE INTENSITIES[a]

Line	Cygni 1986	V827 Her
[Ca VIII]	5.74×10^{-13}	7.48×10^{-13}
[Si VI]	2.28×10^{-12}	1.84×10^{-12}
[Si VII]	2.30×10^{-12}	2.16×10^{-12}
[Al IX][b]	5.89×10^{-13}	7.16×10^{-13}
Brγ	...[c]	7.08×10^{-13}

[a] Units: ergs s^{-1} cm^{-2}; absolute calibration $\pm 5\%$; date: 1987 Aug 29.

[b] Possibly contaminated by He I.

[c] No data.

gor (1988) observed similar emission at 3.28 μm in Nova V842 Cen. Since Pfγ is not apparent in the spectrum, we assume that Pfδ makes a negligible contribution to the feature at 3.28 μm. Physical conditions which may account for the difference between the spectral features of QV Vul and those of the coronal line novae are discussed in § III*f*. The line identifications shown on the spectra are listed in detail in Table 1; peak line intensities are shown in Table 2. Absolute flux calibration for Figure and Table 2 is $\pm 5\%$. Mean 1 σ point-to-point uncertainties averaged over all spectral points in Figure 1 are 3, 3, 311, and 12 mJy for V1819 Cyg, V827 Her, QV Vul, and QU Vul, respectively.

b) *Grating Spectra*

A medium resolution ($\lambda/\Delta\lambda = 920$) *L* band spectrum was taken of Nova QU Vul on 1987 July 27 using the cooled grating array spectrometer (CGAS) of the NASA Infrared Telescope Facility. Absolute flux calibration was determined using BS 7891. The CGAS spectrum is shown in Figure 2. The photometric errors in the CGAS spectra are dominated by seeing fluctuations in the 2''.7 diameter fixed aperture of the spectrometer.

c) *Speckle Interferometry*

Conventional one-dimensional speckle interferometric observations were made of QU Vul at WIRO on 1987 August 2. The data were taken using a resolution $\lambda/\Delta\lambda = 40$ CVF tuned to the wavelength of the 3.20 μm [Mg VIII] coronal line. Observations of the nova, adjacent sky, and a point source (BS 7806) were interleaved in time such that a total of 256 secondary mirror scans were obtained at each position. To cope with the low signal-to-noise ratio in the individual scans, groups of 64 scans were co-added in object space. The resulting four power spectra were then co-added in Fourier space.

Visibility data, along with a best-fit Gaussian, are shown in Figure 3. The applicability of a Gaussian model has been discussed by Ridgway *et al.* (1986). We find that QU Vul is spatially resolved at 0''.6 ± 0''.1 FWHM. The corresponding radius of a spherical emitting region for the line is approximately 1.7×10^{16} cm at an assumed object distance of 3.6 kpc.

III. ANALYSIS

a) *Formation of the Coronal Ions*

Coronal lines are forbidden fine-structure emission lines arising from high ionization states of heavy metals. These low-energy fine-structure transitions of the ground state are excited primarily by electron impact. Relatively low energy ($\sim 10^{-1}$ eV) electrons or weak interaction with high energy electrons can efficiently excite these transitions; however, formation of the ions themselves requires a very energetic environment. The very high stages of ionization which occur in the coronal zone of novae shells can, in principle, result from collisional or photoionization. These states are observed to persist throughout the nova decline and in general are not frozen into the ejecta.

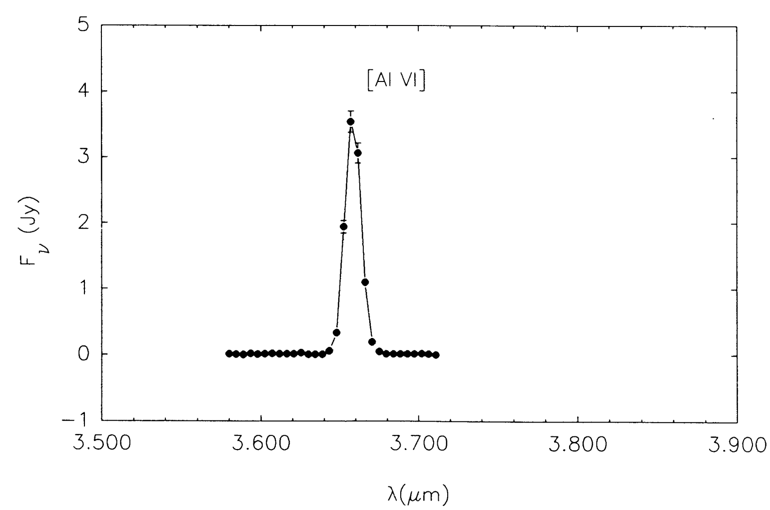

FIG. 2.—A high-resolution *L* band spectrum of Nova QU Vul taken near 3.66 μm. Further details are discussed in § II*b*. Filled circles denote the CGAS detector array elements.

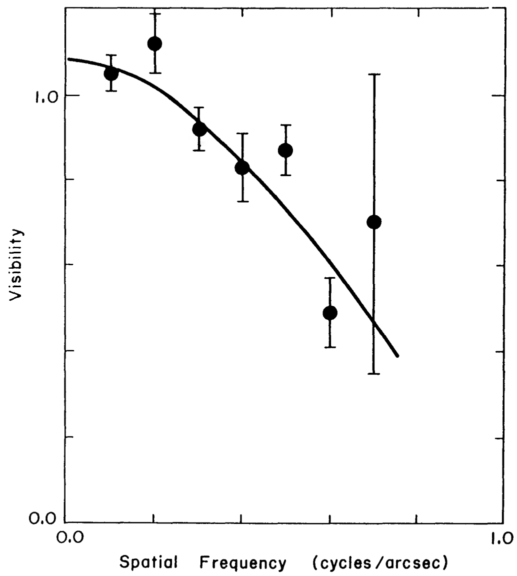

FIG. 3.—Visibility data for Nova QU Vul. The curve shown is a best-fit Gaussian. For comparison, the visibility curve for an unresolved point source is a horizontal line. Further details are discussed in § IIc.

For $n_e > 10^5$ cm^{-3}, the recombination time of the species observed in the near-infrared is short compared to the duration of the coronal line emission phase (see Paper I for a specific example). Coronal zone electron densities of $n_e \sim 10^8$ were derived from optical spectra during the coronal line phase of Nova V1500 Cyg (Ferland and Shields 1978*a*; Ferland, Lambert, and Woodman 1986), while $n_e \sim 10^6$ was derived from radio free-free continuum and infrared coronal line observations during a similar phase of QU Vul (Taylor *et al.* 1987; Paper I). Hence, one can expect that the ionization fraction of an element in the nova shell can be determined by analysis which assumes that a statistical equilibrium between ionization and recombination is achieved. The relative role played by collisional and photoionization in determining the ionization equilibrium of the coronal gas is unknown. Since the ionization equilibrium of a species may be different for these two processes, it is important to know which dominates in order to calculate electron temperatures and elemental abundances in the coronal gas. Some information regarding this question can be gleaned from the near-infrared observations of QU Vul reported in Paper I along with the new data presented here.

We begin by noting that most of the coronal lines observed in V1500 Cyg and QU Vul arise from elements that are highly depleted from the gas phase of the interstellar medium (ISM) of the Galaxy (see, e.g., Seab and Shull 1983). This depletion results from the condensation of dust grains which bind most of the refractory elements of the ISM. The relative temporal development of the coronal and dust condensation zones of novae is unknown except that they are observed to coexist at least temporally in some cases (see Gehrz *et al.* 1986 and Paper I). The size of the coronal emission region measured by speckle interferometry (see § IIc) and the 8×10^{14} cm dust condensation radius measured by Gehrz *et al.* (1986) shows that, in QU Vul, the dust is located within the emitting region of the coronal lines. As a consequence, one cannot assess the importance of photoionization in the shell by comparing the spectra of novae to coronal line planetary nebulae (see Ashley and Hyland 1987 for a spectrum of a coronal line planetary nebula) since the coronal region of the nova ejecta generally will have very different refractory element gas phase abundances due to substantial heavy metal enrichment of the ejecta.

In Paper I, we showed that the coronal lines of QU Vul became apparent in the near-infrared roughly a year after the outburst and persisted for at least 1.3 yr. Therefore, if photoionization plays a significant role in formation of the ions, the source of the ionizing radiation must persist for a significant fraction of the life of the nova to maintain the observed ionization against the relatively short recombination times. This constraint rules out the relatively transient UV radiative precursor of fast shock fronts and leaves direct emission from the nova remnant as the only apparent source of UV photons for ionization of the coronal emitting region.

We can compare the rate of photoionization in the radiation field of the nova remnant at the measured spatial extent of the emitting region to the collisional ionization rate at the electron density derived in Paper I as follows. Let $G(X^i)$ denote the rate of photoionizations of species X from the ith to $(i + 1)$th stage of ionization. Then

$$G(X^i) = \left(\frac{R_*}{r}\right)^2 \int_{\nu T}^{\infty} \frac{\pi B_\nu(T_*)}{h\nu} a(\nu) d\nu \text{ s}^{-1} , \quad (1)$$

where $h\nu_T$ is the threshold energy for ionization of X^i, πB_ν is the Planck function (ergs s^{-1} cm^{-2} Hz^{-1}), $a(\nu)$ is the cross section for photoionization, T_* and R_* are the effective temperature and radius of the nova remnant, and r is the position of interest in the nova shell. Observations of several recent novae with *EXOSAT* reveal that $T_* \simeq 3 \times 10^5$ K and $R_* \simeq 10^9$ cm may be typical of novae remnants during late stages of their outbursts (Ögelman, Krautter, and Beuermann 1987).

Since the coronal gas is in ionization equilibrium, $a(\nu)$ can be found from the rate coefficient for recombination of X^{i+1} to X^i. The recombination rate coefficient is given by

$$\alpha(X^i) = \int_0^{\infty} w\sigma(w) f(w) dw \text{ cm}^3 \text{ s}^{-1} , \quad (2)$$

where $f(w)$ is the electron velocity distribution and $\sigma(w)$ is the cross section for electron capture. Recombination rate coefficients for several species of interest are presented by Shull and Van Steenberg (1982). The cross sections are related by the Milne relation (see, e.g., Osterbrock 1974)

$$\sigma(w) = \left(\frac{g_{ij}}{g_{i1}}\right) \frac{(h\nu)^2}{m_e^2 c^2 w^2} a(\nu) \text{ cm}^2 , \quad (3)$$

where g_{ij} is the statistical weight of the level j into which the recombination occurs and g_{i1} is the statistical weight of the ground state of X^i. We take the ratio of statistical weights as 1 for the purposes of this discussion. We also have that

$$h\nu = E = E_T + \tfrac{1}{2} m_e w^2 , \quad (4)$$

where E_T is the threshold energy for ionization. Taking a Boltzmann distribution for $f(w)$ and substituting equations (3) and (4) into equation (2) yields

$$\alpha(X^i) = \left(\frac{2}{\pi}\right)^{1/2} (m_e k T_e)^{-3/2} c^{-2} \times \exp\left(\frac{E_T}{kT_e}\right) \int_{RT}^{\infty} a(E) E^2 \exp\left(\frac{-E}{kT_e}\right) dE \text{ cm}^3 \text{ s}^{-1} , \quad (5)$$

where T_e is the coronal zone electron temperature. The functional form of $a(E)$ can usually be approximated by

$$a(E) \simeq a_T[\beta(E_T/E)^\eta + (1-\beta)(E_T/E)^{\eta+1}] \quad (6)$$

(see Osterbrock 1974). For a rough approximation, we take $\beta = 1$ and $\eta = 3$, which is appropriate for high ionization states of many heavy elements. We then find using equations (5) and (6) that the cross section at the threshold energy is

$$a_T = (\pi/2)^{1/2} E_T^{-3}(m_e kT_e)^{3/2} c^2 \alpha(X^i) \exp(-E_T/kT_e) I(3)^{-1} , \quad (7)$$

where

$$I(3) = \int_{E_T}^{\infty} E^{-1} \exp(-E/kT_e) dE . \quad (8)$$

Substituting equation (6) into equation (1) yields the final result

$$G(X^i) = a_T v_T^3 \left(\frac{R_*}{r}\right)^2 \int_{v_T}^{\infty} \frac{\pi B_\nu(T_*)}{h\nu^4} d\nu , \quad (9)$$

where a_T is calculated using equation (7).

The radius of the coronal zone of QU Vul measured using the 3.02 μm [Mg VIII] line (§ II*c*) is $r \simeq 10^{16}$ cm. Taking $\alpha(\mathrm{Mg}^{+6}) = 4.94 \times 10^{-11}$ cm^3 s^{-1} (Shull and Van Steenberg 1982), $n_e \sim 10^6$ cm^{-3}, and $T_e \simeq 6 \times 10^5$ K (Paper I), we find $G(\mathrm{Mg}^{+6}) \simeq 2.5 \times 10^{-5}$ s^{-1}. We can now compare this result to the collisional ionization rate.

Collisional ionzation rate coefficients $C(X^i)$ cm^3 s^{-1} for several elements are given by Shull and Van Steenberg. We find that $C(\mathrm{Mg}^{+6}) = 1.44 \times 10^{-11}$ at $T_e = 6 \times 10^5$ K, so that for QU Vul, $n_e C(\mathrm{Mg}^{+6})/G(\mathrm{Mg}^{+6}) \sim 1$. Hence, one can see that collisional and photoionization play roughly equal roles in the formation of this coronal species.

The balance between these two processes also is very sensitive to n_e. For example, at $r = 10^{16}$ cm and $n_e = 10^8$ cm^{-3}, the ionizing photon flux from the nova remnant is reduced by nearly a factor of 2 as a result of Thomson scattering if the ejecta are distributed with constant density along r. Since the balance between $n_e C$ and G is very sensitive to the assumed values of n_e, r, T_*, and R_*, one would expect it to vary greatly from nova to nova. If the relative intensities among the coronal lines are sensitive to this balance, significantly different near-infrared line ratios would be apparent among these objects. However, the near-infrared spectra of each coronal line nova observed to date are remarkably similar (see Fig. 1; Paper I; Grasdalen and Joyce 1980). The [Si VI]/[Si VII] intensity ratio, in particular, is very uniform among these novae. These observations suggest that the measured coronal line ratios do not depend sensitively on the balance between photo- and collisional ionization. The constancy of the [Si VI]/[Si VII] ratio among the known infrared coronal line novae gives us a license to make the simplifying assumption that the ionization equilibrium of the coronal gas can be modeled in terms of collisional ionization.

b) Electron Temperatures and Elemental Abundances

We can now compare the measured ionization equilibrium in the coronal gas to that predicted by models of low-density collisionally ionized plasmas (see, e.g., Jordon 1969; Landini and Monsignori Fossi 1972; Shull and Van Steenberg 1982). This comparison provides a means of determining the electron temperature in the emitting region of the coronal lines, and the elemental abundance of the species which exhibit coronal line emission. We emphasize that the applicability of these results are restricted to the emitting region of the coronal lines. Our working definition of coronal lines is emission lines resulting from ground-state fine-structure transitions of species with $E_T > 100$ eV.

The wide range of ionization states observed in all coronal line novae suggests that at least two distinct emission regions exist in the ejecta of these objects. These are the coronal line emission region and a lower energy H recombination zone. Recombination of the coronal species produces a diffuse field of medium energy $[14 < E_T(\mathrm{eV}) < 100]$ photons which can control the ionization in the H recombination zone of the ejecta which is the emitting region of most of the optical emission lines and all of the lines of H II. All of the dust emission in novae (see, e.g., Gehrz 1988) presumably occurs in this low-energy zone. Physical conditions determined from optical line studies involving species with $E_T \ll 100$ eV may not be applicable to the coronal line emission region. In §§ III*a* and III*e*, we argue that the coronal zone encompasses the dust and most of the lower temperature ejecta.

With these qualifications we can derive the coronal zone electron temperature from the relative intensity of the *K* band Si lines. Neglecting collisional de-excitation and radiative de-excitation into the upper levels of these transitions, one can show that

$$\frac{I_{\mathrm{Si}}^{+6}}{I_{\mathrm{Si}}^{+5}} = \frac{n_{\mathrm{Si}}^{+6}}{n_{\mathrm{Si}}^{+5}} \frac{\nu_{\mathrm{Si}}^{+6}}{\nu_{\mathrm{Si}}^{+5}} \frac{\Omega_{\mathrm{Si}}^{+6}}{\Omega_{\mathrm{Si}}^{+5}} \frac{g_l^{+5}}{g_l^{+6}} , \quad (10)$$

where I_{Si}^{+5} and I_{Si}^{+6} are the measured intensities of the [Si VI] and [Si VII] lines, n_{Si}^{+5} and n_{Si}^{+6} are the number densities of 5 and 6 times ionized silicon, and g_l^i is the statistical weight of the lower level of the transition.

With equation (10) one finds an ionization equilibrium of Si in terms of a measured line ratio. Model collisional ionization equilibria can be used to associate an electron temperature with the value of $n_{\mathrm{Si}}^{+5}/n_{\mathrm{Si}}^{+6}$ measured from the *K* band spectra. A plot of $n_{\mathrm{Si}}^{+5}/n_{\mathrm{Si}}^{+6}$ as a function of T_e is shown in Figure 4. The electron temperature for all four coronal line novae is shown in Table 3. One can see that each nova exhibits nearly the same coronal zone electron temperature of approximately 3×10^5 K.

Elemental abundances can be found by comparing relative coronal line intensities to model ionization equilibria. The line intensity ratio due to emission in two different species X^i and Y^j can be written as

$$\frac{I_x^{+i}}{I_y^{+j}} = \frac{n_x^{+i}}{n_y^{+j}} \frac{\nu_x}{\nu_y} \frac{\Omega_x}{\Omega_y} \frac{g_y}{g_x} . \quad (11)$$

In the case of known T_e, one can find the ionization fraction n^{+i}/n^0 of either element from the model ionization equilibrium

TABLE 3

CORONAL ZONE ELECTRON TEMPERATURE AND ELEMENTAL ABUNDANCES

Object	log T_e (K)	Aluminum N(X)/N(Si)	Magnesium N(X)/N(Si)	Neon N(X)/N(Si)
Sun[a]	...	0.1	0.8	2.5
Cygni 1975[b]	5.46	≥2.1	≥6.7	...[c]
QU Vul[d]	5.47	≥5.6	≥6.6	≥16.0
Cygni 1986	5.44	...[e]	...[e]	...[c]
V827 Her	5.45	...[e]	...[e]	...[c]

[a] Cosmic abundances taken from Allen 1981.
[b] Day 60 line intensities taken from Grasdalen and Joyce 1980.
[c] No *N* band data.
[d] Day 581 and 593 line intensities taken from Greenhouse *et al.* 1988.
[e] No *L* band data.

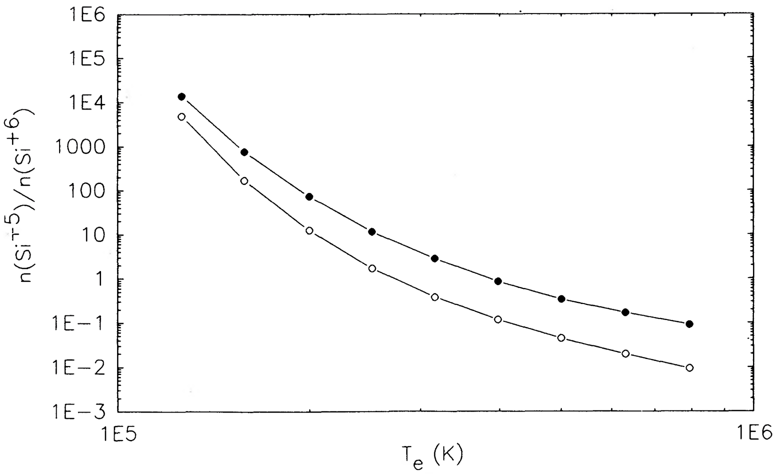

FIG. 4.—Model collisional ionization equilibrium of Si^{+5} and Si^{+6} as a function of electron temperature. Data taken from Jordan (1969) and Shull and Van Steenberg (1982) are shown by filled and open circles, respectively.

so that the measured line ratio I_x^{+i}/I_y^{+j} can be related to the relative abundance n_x^0/n_y^0 of the neutral elements. This relative abundance can then be compared to that expected in a solar abundance pattern. A plot of n^{+i}/n^0 as a function of T_e for various coronal species of interest is shown in Figure 5.

We have that

$$\frac{n_x^0}{n_{\rm Si}^0} = \frac{n_x^{+i}}{n_{\rm Si}^{+j}} \frac{n_{\rm Si}^{+j}}{n_{\rm Si}^0} \frac{n_x^0}{n_x^{+i}} . \tag{12}$$

where $n_x^{+i}/n_{\rm Si}^{+j}$ is determined using equation (11). The results obtained from equation (12) can be very sensitive to which model plasma is used to obtain the two right-hand terms. If $n_{\rm Si}^{+j}/n_{\rm Si}^0$ and n_x^{+i}/n_x^0 are near maximum at the assumed T_e, then this model dependence is reduced (see Fig. 5). In lieu of this uncertainty, the most useful estimate of the relative abundance is the lower limit obtained by evaluating n_x^0/n_x^{+i} at the temperature of maximum ion concentration. The results determined at log $T_e = 5.5$ using [Si VII], [Al VI], [Mg VIII], and [Ne VI] are shown in Table 3. These new results increase the number of novae for which Al and Mg abundances have been determined from two to four (see Truran and Livio 1986).

Diffusion of hydrogen into the white dwarf core and shear mixing at the core–accretion disk boundary have been suggested as mechanisms which result in the heavy metal enrichment observed in these novae and others (see, e.g., Shara 1989, and references therein). Livio and Truran (1987) have suggested that the role of diffusion can be assessed by making abundance determinations for novae with recurrence times which are short compared to the time required for significant diffusion to occur. The near-infrared observations and analysis described here provide a simple technique to carry out this observational test on short recurrence time novae such as T Pyx, U Sco, and others.

In Paper I, we used the models of Jordan (1969) and Landini and Fossi (1972) to calculate Al and Mg abundances. In Table 3, we have used the more recent model by Shull and Van Steenberg (1982) to find lower limits as discussed above. These results are less sensitive to variation in T_e about the assumed value than those presented in Paper I and revise the results reported previously. This revised calculation yields a slightly higher aluminum and magnesium abundance, and a lower electron temperature than reported previously. One can see

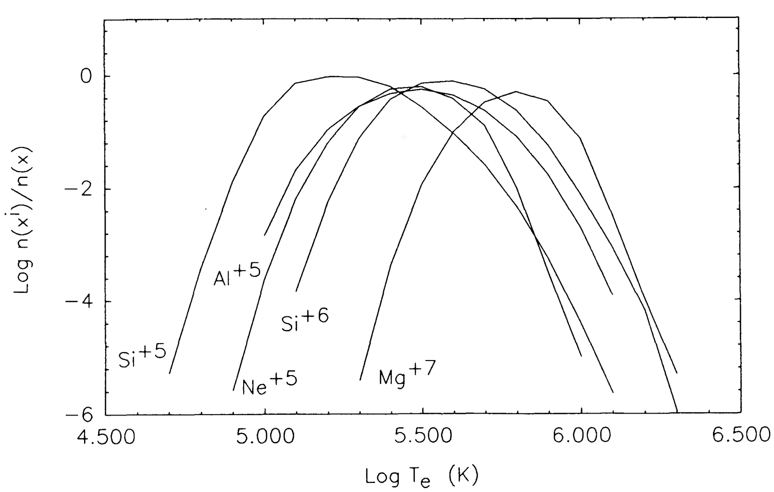

FIG. 5.—Model collisional ionization equilibrium of coronal species as a function of electron temperature. Data for Al were taken from Landini and Monsignori Fossi (1972). Data for the remaining elements were taken from Shull and Van Steenberg (1982).

that both coronal line novae which were observed at L exhibit similar abundance patterns in these elements.

c) *Ionization Structure of the Ejecta*

A very wide range of ionization states is observed in novae shells. Many low- and medium-energy ions are typically observed along with coronal lines in novae (see, e.g., Sanford 1946; Grasdalen and Joyce 1976; Wallerstein and Garnavich 1986; Paper I). This range of ionization can, in part, be explained by nonuniform expansion of the shell.

Many parameters which control the ionization equilibrium of the ejecta and the intensity of transitions of the resulting ions (e.g., photoionization cross sections and collision strengths) are functions of the nuclear charge Z and, hence, can be extrapolated along isoelectronic sequences. An isoelectronic sequence of elements is a sequence of increasing nuclear charge Z and constant electronic charge. The sequences are named for their neutral member. So for example, the fluorine isoelectronic sequence consists of F, Ne^{+1}, Na^{+2}, Mg^{+3}, Al^{+4}, Si^{+5}, etc. Several coronal lines observed in QU Vul and others arise from members of this sequence. The wavelength of a specific fine-structure transition is often a smooth function of Z among elements of a specific sequence (see, e.g., Edlén 1969; White 1934). This relationship is illustrated by Figure 6, which shows the wavelength of the $2s^2\,2p^5\,{}^2P_{1/2}$–${}^2P_{3/2}$ transition as a function of Z in members of the F and B isoelectronic sequences. The data for the figure were taken from Edlén. This type of analysis was used as an important tool to identify coronal lines in the Sun and is largely the key to understanding the coronal line spectra of novae.

Grasdalen and Joyce (1976) observed a number of near-infrared coronal lines in V1500 Cyg. The species identified were unexpected in the infrared spectra of novae. Although high ionization states are typically seen in the optical, the $\Delta J = 1$ ground-state fine-structure transitions which we observe in the near-infrared are rarely observed in optical spectra. This observation is surprising since these low-energy transitions would always be excited in a nova shell, and the elements which would exhibit them at optical wavelengths are not thought to be under abundant in novae ejecta. In the remainder of § III*c*, we expand on Grasdalen and Joyce's analysis of V1500 Cyg (unpublished) in lieu of results obtained on recent novae. To understand the relevance of Figure 6 to the spectral evolution of novae, we begin by clearly defining two terms which are not in widespread use in all areas of astronomy.

The *critical density*, $n_{\rm crit}$, of a transition is the electron density at which the rates of collisional and radiative deexcitation of the upper level of the transition are equal. When $n_e \gg n_{\rm crit}$, the transition is said to be thermalized. The forbidden coronal lines are conspicuous only when $n_e \ll n_{\rm crit}$. For a transition from $j \rightarrow k$, the critical density of the level j is given by

$$n_{\rm crit} = \frac{m_e^{3/2}}{\hbar^2}\left(\frac{kT_e}{2\pi}\right)^{1/2}\frac{\sum_{k<j} A_{jk}}{\sum_{k\neq j}\Omega_{jk}}\,g_j\ {\rm cm}^{-3}\,, \tag{13}$$

where Ω is the collision strength of the transition, and A is the spontaneous transition probability. Transition probabilities for a number of coronal species have been calculated by Kafatos and Lynch (1980), and a complete list has been compiled by Kaufman and Sugar (1986).

For a gas in ionization equilibrium, each species X^i has an electron temperature at which its abundance is a maximum (see Fig. 5). This temperature is often called the *characteristic temperature* of the ion which we denote as $T_c(X^i)$. If the ionization equilibrium is dominated by collisional ionization so that $n_e\,C(X^i) \gg G(X^i)$ for all X^i of interest, then $T_c(X^i)$ is independent of n_e. The applicability of this case is discussed in § III*a*. Values of $T_c(X^i)$ have been calculated for collisional ionization of most elements of interest (see references to model collisionally ionized gas in § III*b*).

We can now use equation (13) to calculate $n_{\rm crit}$ for the $2s^2\,2p^5\,{}^2P_{1/2}$–${}^2P_{3/2}$ transition of each member of the F isoelectronic sequence (see Fig. 6) at its characteristic temperature. Collision strengths can be found in Osterbrock (1974) and Blaha (1969) and can be interpolated along the F sequence. The result is shown in Figure 7 taken from Grasdalen and Joyce (1980). Each data point is labeled with the name of the ion and the wavelength of the above fine structure line in that ion. The curve connecting the data points serves as a visual aid.

One can immediately see from Figures 6 and 7 that very high stages of ionization must be achieved in order that the transitions observed in the near-infrared have optical counterparts.

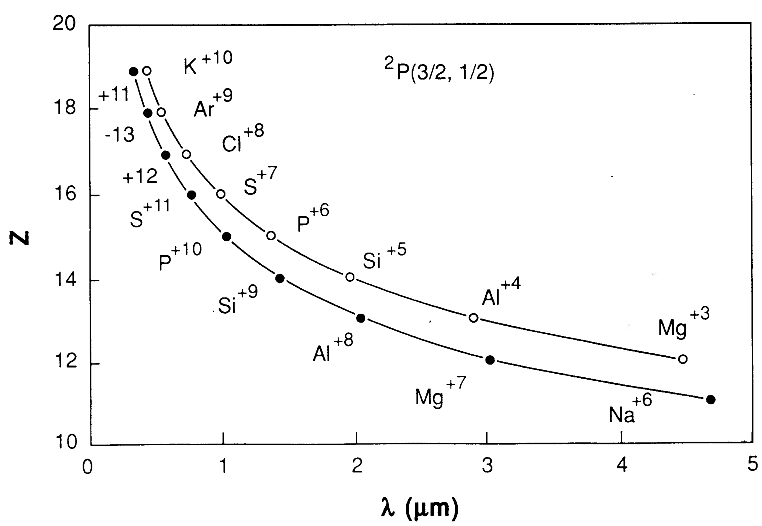

FIG. 6.—The wavelength of the ${}^2P_{3/2}$–${}^2P_{1/2}$ transition among elements of the F (*open circles*) and B (*filled circles*) isoelectronic sequences

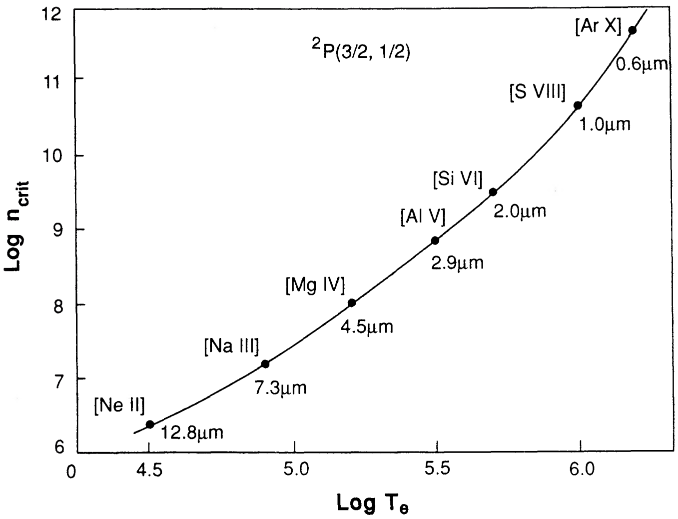

FIG. 7.—Taken from Grasdalen and Joyce (1980), elements of the F isoelectronic sequence are plotted at their characteristic temperatures and at the critical density for the $^2P_{3/2}$–$^2P_{1/2}$ transition in each ion. The wavelength of the transition is shown below each species. The $n_{\rm crit}$, T_e parameter space for coronal line emission due to F sequence elements is restricted to the region below the curve.

For any stage of ionization *i*, this emission line will be observed primarily when n_e and T_e are restricted to the parameter space below the curve shown in Figure 7. Since the ejecta are expanding and also cooling as a result of line radiation, n_e and T_e decrease with time after the outburst. During the expansion, electrons are always abundantly available to excite this fine-structure transition. But as the expansion proceeds, collisional de-excitation decreases in species of decreasing E_T while the abundance of high ionization states decreases as a result of decreasing T_e relative to $T_c(X^i)$ for the large E_T species. Hence, the wavelength range over which this transition is exhibited *shifts longward* with increasing expansion of the nova shell.

The largest E_T species observed is determined primarily by the highest temperature achieved during the optically thin phase of the novae decline. Since the ejecta blend into the local interstellar medium, a wide range of n_e can always be assumed to exist in novae shells. Therefore, as the ejecta cools, we expect each isoelectronic sequence observed to be observationally complete below the highest E_T species observed in each sequence.

If the expansion is very nonuniform, an ejecta shell with less than spherical symmetry exhibiting a wide range of n_e and T_e will result. As shown in Figure 7, a wide range of ionization states X^i will be traced by each ground state fine structure transition observed. The wavelength of the transition in each X^i will predominantly occur throughout the near- and thermal-infrared. Extreme conditions ($T_e > 10^6$, $n_e < 10^{12}$) can result in the infrared transitions having optical counterparts (see, e.g., Wallerstein and Garnavich 1986); however, the visual band is clearly not an optimal wavelength range in which to distinguish this class of novae.

These ideas are consistent with all observations of coronal line novae that we are aware of. Important points of comparison include the following:

1. For the coronal line novae observed at K and L to date, each observed transition (see Table 1) of an ion is represented by *all* of the members of the isoelectronic sequence which is uniquely associated with it and for which the transition would be in band (see Fig. 1 and references to V1500 Cyg and QU Vul discussed above). If one separates the observed species into isoelectronic sequences, the resulting sequences are observationally complete for the wavelength range covered by the spectra. Although the range of infrared wavelengths which have been explored spectroscopically exclude the J (1.2 μm), H (1.6 μm), and M (4.9 μm) bands, agreement with the available spectra is remarkable.

2. Excess N band emission was observed in V1500 Cyg (see, e.g., Ferland and Shields 1978*b*) and extremely intense [Ne II] 12.8 μm emission was observed in Nova QU Vul (see Gehrz, Grasdalen, and Hackwell 1985). Ferland and Shields suggested that the N band excess in V1500 Cyg was due to [Ne II] emission. Separating the near-infrared coronal species into isoelectronic sequences reveals the relationship between the [Ne II] 12.8 μm line and the K and L band coronal lines of V1500 Cyg (see Fig. 7). One would expect that novae which exhibit $^2P(3/2, 1/2)$ transition of F sequence coronal species to also exhibit this transition in [Ne II] when other low E_T species are present since a suitably low-density ($n_e < n_{\rm crit}$) region will always exist in the outer regions of the ejecta. This expectation is consistent with the data obtained for V1500 Cyg and provides additional circumstantial evidence that the N band excess of V1500 Cyg was due to [Ne II] emission at 12.8 μm. Similarly, we expect coronal line novae to be strong sources of [C II] 157.7 μm emission since we expect the B sequence to be observationally complete and carbon is typically overabundant in novae.

3. Optical line profiles of QU Vul suggest that the expansion velocity is nonuniform and high-resolution VLA images of the ejecta reveal that the shell is only axisymmetric (Wagner 1987; Taylor *et al.* 1987) in agreement with the wide range of T_e and n_e implied by comparison of the characteristic temperature and critical density of the highest and lowest E_T coronal species observed. Gradients in T_e and n_e may be constrained by hydrodynamic modeling of the ejecta. The observed range of these parameters which can be inferred from the observed range of $T(X^i)$ and $n_{\rm crit}$ among coronal line emitting species may provide model constraints for such efforts.

4. Independent determinations of n_e for novae exhibiting coronal line emission (see references concerning n_e in § III*a*) are consistent with the idea that $n_e < n_{\rm crit}$ for the coronal species observed. Measurements of n_e and T_e in infrared coronal line novae to date suggest that in lieu of Figures 6 and 7 (and their analogs for other sequences) optical coronal lines will be only occasionally present when infrared coronal lines are prominent.

5. Electron temperatures determined from optical coronal lines such as [Ar X] and [Ar XI] in Nova RS Oph 1985 (see Wallerstein and Garnavich 1986) are in excess of 10^6 K, in agreement with the parameter space shown in Figure 7.

This analysis provides a very powerful tool for analyzing nova spectra. For example, the $^2P(1/2, 3/2)$ line was observed among members of the F isoelectronic sequence ([Al V], [Si VI], and [Ne II]) in QU Vul. Therefore, we predict that if this nova had been observed at M, one would see emission from this transition in [Mg IV] at $\lambda_{\rm lab} = 4.492$ μm (see Fig. 6). We are aware of no other analysis which would allow one to make such a specific prediction among emission lines of different elements.

d) The Role of Shocks for Formation of the Ions

The interaction of a strong shock ($V_s \sim 180$ km s^{-1}) with the ejecta of QU Vul was observed as a radio continuum outburst by Taylor *et al.* (1987) on day 206 of the nova. In Paper I, we showed that approximately 100 days elapsed between the passage of the shock and the appearance of coronal lines within the L band. We concluded that as a result of this delay the shock was not closely related to the formation of the coronal zone. In light of arguments discussed in § III*c*, we now find that an alternate interpretation is more likely.

If the shock observed by Taylor *et al.* produced the coronal ionization, then optical spectra of QU Vul taken at or slightly after day 206 of the nova may show coronal lines. Optical spectra of QU Vul exist for various dates between days 261 and 927 (Wagner 1987; Andrillat 1987). The very large i species (e.g., Fe XI) are not apparent in the spectra until day 491 (Andrillat 1987), roughly 9 months after the passage of the shock and 5 months after the L band lines became prominent. The very coarse temporal observations which exist make it difficult to construct an accurate picture of the spectral evolution of QU Vul, and the precise times of maximum brightness of the various lines observed are unknown as a consequence. However, it seems clear that a substantial time period elapsed between the radio continuum outburst and the appearance of the coronal lines. Line intensities presented in Paper I and those obtained by Andrillat (1987) show that several species ([Mg VIII], [Si IX], [S VIII]) exhibited maximum line intensity nearly a year after the radio outburst. The arguments of § III*c* provide a basis for understanding this time delay.

If the radio continuum outburst is related to the formation of the coronal emitting region, then the time which elapsed between the outburst and the appearance of the coronal lines is the time required for T_e and n_e in the postshock gas to enter the parameter space shown in Figure 7. This measured time interval may form a useful model constraint.

For uniform shell expansion, and a specific fine structure transition, one would expect to see a time progression from optical to infrared coronal line emission. The sequence of species (X^i) revealed could be grouped into isoelectronic sequences of the sort shown in Figure 6. If the initial ionization up to some fixed i occurs at high density, a time period will elapse during which no coronal emission will be apparent. The progression of coronal lines will begin when $n_e < n_{\rm crit}$ for the largest E_T species present in the ejecta. This progression is known to extend to the mid-infrared neon lines and may extend to B sequence species such as [O IV] 25.9 μm and [C II] 157.7 μm. We stress the need for far-infrared spectra of novae.

For any real nova, large temperature and density gradients are likely to exist in the shell throughout the expansion. As a consequence, the simple temporal evolution described above may be difficult to observe. But even in the case of very nonuniform expansion, we predict that *all* of the coronal species observed could be separated into a set of isoelectronic sequences such that each set would be complete for the observed wavelength range.

e) *Expansion of the Emitting Region*

A number of techniques have been used to determine the expansion velocity of QU Vul in its latter stages of decline. QU Vul was spatially resolved by VLA radio continuum imaging (Taylor *et al.* 1987) on days 289 and 497 of the nova. The radio continuum images reveal that the nova shell is elongated. One finds an expansion velocity of 940–1600 km s^{-1} for the major and minor axis of the shell respectively from comparison of these images and an assumed object distance of 3.6 kpc. An expansion velocity determined from the temporal development of the coronal line intensities between days 581 and 733 was presented in Paper I as 752 km s^{-1}. Finally, the [Al VI] line in QU Vul was velocity-resolved on day 919 of the nova by the resolution $\lambda/\Delta\lambda = 920$ CGAS spectra shown in Figure 2. The FWHM of a Gaussian fit to the line profile is 418 $\pm$ 132 km s^{-1}.

TABLE 4

CORONAL ZONE EXPANSION VELOCITY OF QU VULPECULAE

Day	$V(10^3$ km s$^{-1})$	References
140	5–7[a]	1
289–497	0.9–1.6	2
581–733	0.75	3
919	0.42[a]	4

[a] FWHM.

REFERENCES.—(1) Gehrz *et al.* 1985; (2) Taylor *et al.* 1987; (3) Greenhouse *et al.* 1988; (4) this paper.

The overall picture of the expansion velocity of QU Vul is shown in Table 4. To interpret the results one must note that the *detailed* spatial relationship of the coronal and H recombination zones of the nova shell is unknown. Since the free-free radio continuum emission is proportional to $T_e^{-3/2}$, the radio continuum images will be dominated by emission from the H recombination zone (which is also the emitting region for [Ne II]) while the coronal line measurements are insensitive to this lower temperature emitting region. The various velocity measurements which have been produced for QU Vul should be compared with this distinction in mind. It seems clear from the results listed in Table 4 that some real deceleration of the total ejecta occurred between the time of the [Ne II] measurement of Gehrz, Grasdalen, and Hackwell 1985 and the time of pronounced coronal line emission. Deceleration of novae ejecta is often observed (cf. Duerbeck 1987) and presumably results from momentum transfer between the ejecta and the local interstellar medium.

The ejecta of QU Vul were spatially resolved by speckle interferometry of the 3.02 μm [Mg VIII] line (§ II*c*) on day 925 of the nova. If we allow the major axis shell diameter measured in the radio continuum on day 497 to expand at its apparent velocity of 1.6×10^3 km s^{-1}, we find that the shell spatial extent projected to day 925 is in reasonable agreement with the shell size measured by speckle interferometry. Comparison of these results show that the emitting region of the coronal lines is at least as extensive as the H recombination zone of the ejecta.

f) *Frequency of Coronal Line Outbursts*

Roughly a decade elapsed between the discovery of coronal line emission in V1500 Cyg and QU Vul which would suggest that infrared coronal line novae are relatively rare. Since three of four novae recently studied were found to be infrared coronal line novae, we suspect that novae of this class are not rare. However, the spectrum of QV Vul and perhaps V1370 Aql (Bode and Evans 1984) indicates that all bright novae do not exhibit this emission.

Coronal line novae observed to date have not developed optically thick dust shells, presumably because the shell gas density is generally less than the critical density for dust condensation (see Gehrz and Ney 1987). Novae such as QU Vul and V1370 Aql, which form substantial dust, presumably have coronal zone electron densities which lie outside the parameter space shown in Figure 7. The 3.28 μm emission feature of QV

Vul reveals that atomic carbon can form hydrocarbon molecules in the hard UV field of the nova remnant at electron densities that are probably above the curve in Figure 7.

Alternatively, dusty novae may have coronal line emission that is difficult to observe. The increased continuum background associated with dust formation can mask line emission especially to low spectral resolution measurements (see, e.g., Gehrz 1988, p. 389). In addition, coronal ionization may be rapidly quenched as a result of radiative cooling by the dust resulting in a very short coronal line emission phase.

Although infrared coronal line novae may be relatively common, in absolute terms, less than a dozen novae have been observed spectroscopically at the wavelengths of the Al, Mg, and Ne lines listed in Table 1 (see, e.g., Bode 1989). Only a few more have been well studied in the 2.2 μm window. Unfortunately, this very small sample size does not form a sufficient data base to determine the frequency of occurrence of a coronal line emission phase in novae. Similarly, models that predict the ratio of ONeMg to CO novae cannot be tested by existing observations since only a handful of novae have had abundances in Al, Mg, and Ne determined, and selection effects (see Starrfield, Sparks, and Truran 1986) may favor the discovery of ONeMg novae.

IV. SUMMARY

Near-infrared spectroscopic monitoring of bright novae have distinguished a group of novae which exhibit remarkably similar infrared spectra. The spectra suggest that the ejecta of these novae are overabundant in aluminum, magnesium, and neon relative to the Sun. In each case, the emitting region of the highly ionized heavy elements which dominate the near-infrared spectra of these objects is characterized by an electron temperature of approximately 3×10^5 K.

Aluminum, magnesium, and neon abundances have been determined for two of the four known infrared coronal line novae. The results suggest that coronal line novae, as a group, may be related to ONeMg novae. These new results provide increased observational evidence for ONeMg outbursts and provide a simple technique for determining abundances of Al, Mg, and Ne from near-infrared spectra.

One of the four known infrared coronal line novae (QU Vul) has been spatially resolved. The results reveal that the emitting region of the coronal lines encompasses the principal ejecta of the nova. The measured size, temperature, and density of the QU Vul ejecta shell suggests that photoionization alone is insufficient to account for the observed spatial extent of the coronal emitting region. The uniformity among the K band spectra of all coronal line novae suggests that the coronal line ratios are insensitive to the balance between photo- and collisional ionization within the ejecta.

Separating the observed coronal species into isoelectronic sequences allows one to understand the relationship between the coronal emission lines and the changing physical conditions within the expanding nova shell. Since the coronal line transitions are always excited, one expects a given sequence to be observationally complete for the wavelength range observed. This expectation allows one to use the observation of only a few near-infrared coronal lines to precisely predict the presence of coronal lines due to different elements which occur over a wide range of wavelengths and outside of ground-based atmospheric windows. Hence, this analysis can greatly increase the productivity of more difficult mid-infrared and airborne spectroscopic studies of novae with the result that the range of elements for which coronal zone abundances can be determined is extended.

We emphasize the need for increased spectroscopic observation of novae from far-red to far-infrared wavelengths in addition to near-infrared spectra which are temporally well sampled throughout novae decline. The elemental abundances determined for coronal line novae suggest that they are related to ONeMg novae. Velocity-resolved spectra of coronal line novae are necessary to further explore this relationship. A high spectral resolution search for coronal line emission in novae which form thick dust shells is also desired to explore the relationship between the minimum density for dust condensation and the maximum density for coronal line emission in novae shells.

We thank A. Tokunaga for assistance with the observations made with CGAS, and H. A. Thronson, H. M. Dyck, and S. Starrfield for a number of useful comments. M. A. G. was supported by NASA grant NAG2-134. G. L. G. and C. E. W. were supported in part by USAF grant AFOSR-88-0057. R. D. G. was supported by NSF, USAF, and the University of Minnesota Graduate School.

REFERENCES

Allamandola, L. J., Tielens, A. G. G. M., and Barker, J. R. 1987, in *Interstellar Processes*, ed. D. J. Hollenbach and H. A. Thronson (Dordrecht: Reidel), p. 471.
Allen, C. W. 1981, *Astrophysical Quantities* (3d ed.; London: Athlone).
Andrillat, Y. 1987, private communication.
Ashely, M. C. B., and Hyland, A. R. 1988, *Ap. J.*, **331**, 532.
Black, J. H., and Gallagher, J. S. 1976, *Nature*, **261**, 296.
Blaha, M. 1969, *Astr. Ap.*, **1**, 42.
Bode, M. 1989, in *Infrared Spectroscopy in Astronomy, Proc. 22nd Eslab Symposium*, in press.
Bode, M. F., and Evans, A. 1984, *M.N.R.A.S.*, **207**, 897.
Borghesi, A., Bussoletti, E., and Colangeli, L. 1987, *Ap. J.*, **314**, 442.
De Muizon, M., Geballe, T. R., D'Hendecourt, L. B., and Bass, F. 1986, *Ap. J.* (*Letters*), **306**, L105.
Duerbeck, H. W. 1987, *Ap. Space Sci.*, **131**, 461.
Duley, W. W., and Williams, D. A. 1986, *M.N.R.A.S.*, **219**, 859.
Edlén, B. 1969, *Solar Phys.*, **9**, 439.
Ferland, G. J., Lambert, D. L., and Woodman, J. H. 1986, *Ap. J. Suppl.*, **60**, 375.
Ferland, G. J., and Shields, G. A. 1978*a*, *Ap. J.* (*Letters*), **224**, L15.
———. 1978*b*, *Ap. J.*, **226**, 172.
Gallagher, J. S., and Starrfield, S. 1978, *Ann. Rev. Astr. Ap.*, **16**, 171.
Gehrz, R. D. 1988, *Ann. Rev. Astr. Ap.*, **26**, 377.
Gehrz, R. D., *et al.* 1986, *Ap. J.* (*Letters*), **308**, L63.
Gehrz, R. D., Grasdalen, G. L., and Hackwell, J. A. 1985, *Ap. J.* (*Letters*), **298**, L47; **306**, L49.
———. 1987, in *Encyclopedia of Phys. Sci. and Tech.* (New York: Academic), p. 53.
Gehrz, R. D., and Ney, E. P. 1987, *Proc. Nat. Acad. Sci.*, **84**, 6961.
Grasdalen, G. L., and Joyce, R. R. 1976, *Nature*, **259**, 187.
———. 1980, preprint.
Greenhouse, M. A. 1987, *IAU Circ.*, No. 4398.
Greenhouse, M. A., Grasdalen, G. L., Hayward, T. L., Gehrz, R. D., and Jones, T. J. 1988, *A.J.*, **95**, 172; **98**, 738 [1989] (Paper I).
Greenhouse, M. A., Woodward, C. E., Seaman, R., and Poczulp, G. 1987, *IAU Circ.*, No. 4449.
Hyland, A. R., and McGregor, P. J. 1988, in *IAU Symposium 135, Interstellar Dust*, ed. L. J. Allamandola (Dordrecht: Reidel), in press.
Jordan, C. 1969, *M.N.R.A.S.*, **142**, 501.
Kafatos, M., and Lynch, J. P. 1980, *Ap. J. Suppl.*, **42**, 611.
Kaufman, V., and Sugar, J. 1986, *J. Phys. Chem. Ref. Data*, **15**, 331.
Lambert, D. L., and Hinkle, K. H. 1984, *Pub. A.S.P.*, **96**, 222.
Landini, M., and Monsignori Fossi, B. C. 1972, *Astr. Ap. Suppl.*, **7**, 291.
Livio, M., and Truran, J. W. 1987, *Ap. J.*, **318**, 316.
Ögelman, H., Beurermann, K., and Krautter, J. 1984, *Astr. Ap.*, **177**, 110.
Osterbrock, D. E. 1974, *Astrophysics of Gaseous Nebulae* (San Francisco: Freeman).

Ridgway, S. T., Joyce, R. R., Connors, D., Pipher, J. L., and Dainty, C. 1986, *Ap. J.*, **302**, 662.
Sakata, A., Wada, S., Tanabe, T., and Onaka, T. 1984, *Ap. J. (Letters)*, **287**, L51.
Sanford, R. F. 1946, *Pub. A.S.P.*, **59**, 334.
Seab, C. G., and Shull, M. J. 1983, *Ap. J.*, **275**, 652.
Shara, M. M. 1989, *Pub. A.S.P.*, **101**, 5.
Shull, M., and Van Steenberg. 1982, *Ap. J. Suppl.*, **48**, 95; **49**, 351 [1982].
Smith, H. A., Larson, H. P., and Fink, U. 1981, *Ap. J.*, **244**, 835.
Snijders, M. A. J., Batt, T. J., Roche, P. F., Seaton, M. J., Morton, D. C., Spoelstra, T. A. T., and Blades, J. C. 1987, *M.N.R.A.S.*, **228**, 329.
Starrfield, S., Sparks, W. M., and Truran, J. W. 1986, *Ap. J. (Letters)*, **303**, L5.
Taylor, A. R., Seaquist, E. R., Hollis, J. M., and Pottasch, S. R. 1987, *Astr. Ap.*, **183**, 38.
Truran, J. W., and Livio, M. 1986, *Ap. J.*, **308**, 721.
Wagner, R. M. 1987, private communication.
Wallerstein, G., and Garnavich, P. M. 1986, *Pub. A.S.P.*, **98**, 875.
White, H. E. 1934, *Introduction to Atomic Spectra* (New York: McGraw-Hill), p. 331.
Williams, R. E., Ney, E. P., Sparks, W. M., Starrfield, S., and Truran, J. W. 1985, *M.N.R.A.S.*, **251**, 221.

J. Benson, G. L. Grasdalen, and C. E. Woodward: Wyoming Infrared Observatory, University of Wyoming, Box 3905 University Station, Laramie, WY 82071

R. D. Gehrz: Astronomy Department, University of Minnesota, 116 Church Street S.E., Minneapolis, MN 55455

M. A. Greenhouse: Laboratory for Astrophysics, National Air and Space Museum, Smithsonian Institution, Washington, DC 20560

E. Rosenthal: Institute for Astronomy, University of Hawaii, 2680 Woodlawn Drive, Honolulu, HI 96822

M. F. Skrutskie: Department of Physics and Astronomy, University of Massachusetts, Amherst, MA 01002